

The study of polycrystalline  $\text{PbMg}_{1/3}\text{Nb}_{2/3}\text{O}_3$  by the electron paramagnetic resonance of  $\text{Fe}^{3+}$  ions

This article has been downloaded from IOPscience. Please scroll down to see the full text article.

1994 J. Phys.: Condens. Matter 6 3421

(<http://iopscience.iop.org/0953-8984/6/18/018>)

View [the table of contents for this issue](#), or go to the [journal homepage](#) for more

Download details:

IP Address: 171.66.16.147

The article was downloaded on 12/05/2010 at 18:20

Please note that [terms and conditions apply](#).

## The study of polycrystalline $\text{PbMg}_{1/3}\text{Nb}_{2/3}\text{O}_3$ by the electron paramagnetic resonance of $\text{Fe}^{3+}$ ions

Maya D Glinchuk, Vladislav Skorokhod, Igor P Bykov, Vilnis Dimza† and Eva Černošková‡

Institute for Materials Science, Academy of Sciences of Ukraine, 3 Krzhizhanovski Street, Kiev 252180, Ukraine

Received 1 September 1993, in final form 3 December 1993

**Abstract.** EPR spectra of PMN ceramics doped with 0.1 mol%  $\text{Fe}_2\text{O}_3$  were recorded at  $T = 100$  K and  $T = 475$  K and were attributed to  $\text{Fe}^{3+}$  ions in positions with different local symmetries. Three types of  $\text{Fe}^{3+}$  paramagnetic centres of rhombic, axial and cubic symmetry in average and individual low-symmetry fluctuations were described by spin Hamiltonians with distributed constants. The other type of centre at  $T = 100$  K was found to retain the pure cubic symmetry of ideal homogeneous regions. The superhyperfine interaction between  $\text{Fe}^{3+}$  and neighbouring  $^{207}\text{Pb}$  nuclei is 4 mT. The mechanisms by which the paramagnetic centre symmetry is decreased involves a contribution from the cation disorder in B sites and a temperature-dependent contribution of lattice distortions in polar regions. The oxygen sublattice shift was estimated.

### 1. Introduction

$\text{PbMg}_{1/3}\text{Nb}_{2/3}\text{O}_3$  (PMN) is one of the most intensively studied relaxor ferroelectrics. Information on its local structure, ion positions and dynamics in a wide temperature range was recently obtained from x-ray and neutron diffraction data by Bonneau *et al* (1991). NMR data obtained by Laguta *et al* (1990) and Glinchuk *et al* (1991) revealed information on the ion displacement, the peculiarities of the dynamics and the existence of the ideal homogeneous 1:2 structure in PMN (figure 1).

The high sensitivity of the EPR method to the structure distortions, the ion displacement and the distribution of internal fields is of great importance for its application to PMN, whose main feature is the coexistence of electric dipole moments of displaced atoms, resulting in the occurrence of polar regions and random internal fields induced by locally non-compensated charges.

In this paper an EPR investigation of PMN ceramics was carried out for the first time. The EPR spectra of the paramagnetic probe  $\text{Fe}^{3+}$  were observed at  $T = 100$  K and  $T = 475$  K. Four types of paramagnetic centre were attributed to  $\text{Fe}^{3+}$  positions in regions with different local symmetries.

† Present address: Institute of Solid State Physics, University of Latvia, 8 Kengaraga Street, Riga 226063, Latvia.

‡ Present address: Technical University of Chemistry and Technology, CS Legii Nam. 565, 532 10 Pardubice, Czech Republic.

## 2. Experimental details

PMN ceramic specimens with 0.1 mol% Fe<sub>2</sub>O<sub>3</sub> were prepared by two-stage hot pressing. Details of this technology have been described by Dimza *et al* (1989).

The EPR spectra were measured with an ERS-200 spectrometer. The experimental conditions were as follows: frequency, 9.35 GHz; temperature, 100–475 K. The EPR spectra were unobservable in the temperature region of the PMN permittivity maximum (200–300 K) owing to dielectric losses in the microwave circuit.

The spectra at  $T > 300$  K and  $T < 200$  K strongly differed but, within the high- and low-temperature regions of measurements, only the EPR signal amplitude varied. So we found sufficient data to show in figure 2 only spectra at  $T = 100$  K and  $T = 475$  K. The arrows indicate the characteristic parts of the spectra and their effective  $g'$ -values ( $g' = h\nu/\beta H$ ). Details of the narrow line at  $g' = 2$  at 100 K are shown in figure 3.

## 3. EPR spectra and their description

### 3.1. Rhombic Fe<sup>3+</sup> centres

Plots of  $g'$  versus  $E/D$ , where  $D$  and  $E$  are constants of the spin Hamiltonian

$$\mathcal{H} = g\beta H + DS_x^2 + E(S_x^2 - S_y^2) \quad (1)$$

for d<sup>5</sup> ions in a strong crystal field ( $|D| \gg g\beta H$  and  $|E| \gg g\beta H$ ), were calculated by Wickman *et al* (1963). It is seen that the strong line at  $g' = 4.3$  belongs to Fe<sup>3+</sup> in a strong crystal field with complete rhombic symmetry ( $3|E| = |D|$ ). Special attention should be drawn to the specific diffused form of the  $g' = 4.3$  line. This lineshape was obtained by simulation of Fe<sup>3+</sup> centres in structurally disordered polycrystalline solids performed by Kliava (1986) on the assumption that the constants  $D$  and  $E$  have the two-dimensional Gaussian distribution

$$P(D, E) = \frac{1}{\pi \Delta D \Delta E \sqrt{1 - \rho^2}} \exp \left\{ -\frac{1}{1 - \rho^2} \left[ \left( \frac{D - D_0}{\Delta D} \right)^2 + 2\rho \frac{D - D_0}{\Delta D} \frac{E - E_0}{\Delta E} + \left( \frac{E - E_0}{\Delta E} \right)^2 \right] \right\}. \quad (2)$$

Distribution of the  $g$ -tensor components and constants of the fourth and higher orders is supposed to result in a much lower magnetic field deviation than the  $D$  and  $E$  distribution. It may be taken into account by the width  $\Delta H$  of an individual line as a simulation parameter. Patterns of spectra calculated by Kliava (1986) are notably sensitive to variations in the distribution (2) parameters, for instance the higher  $D_0$  magnitude of the flatter peaks of the  $g' = 4.3$  line. We managed to find two simulated spectra with details close to our experimental  $g' = 4.3$  lines at 100 and 475 K. This made it possible to estimate parameters of the distribution (2):  $D_0^{(rh)} = 0.4$  cm<sup>-1</sup> at 100 K and  $D_0^{(rh)} = 0.6$  cm<sup>-1</sup> at 475 K. At both temperatures,  $E_0^{(rh)} = \frac{1}{3}D_0^{(rh)}$ ,  $\Delta D^{(rh)} = 0.1$  cm<sup>-1</sup>,  $\Delta E^{(rh)} = 0.035$  cm<sup>-1</sup> and  $\Delta H = 2$  mT. All  $D_0$  and  $E_0$  are given in absolute values; the superscript (rh) indicates that the constants belong to rhombic centres.

### 3.2. Axial $Fe^{3+}$ centres

The stair-like parts of the spectra at  $g' = 6-8$  at both temperatures do not belong to the rhombic centres described above. These spectra have no singularities and weakly depend on the temperature. It follows from plots of  $g'$  versus  $E/D$  for  $d^5$  ions in a strong crystal field by Wickman *et al* (1963) that the lowest Kramers doublet of centres with a symmetry near to complete rhombic ( $E \simeq \frac{1}{3}D$ ) gives a response at  $g' = 8-10$ . Meanwhile, the region of  $g' = 6-8$  corresponds to centres with  $E/D = 0-0.1$ . So the star-like spectrum involves responses from a set of centres with very close constants varying as stated above. We may ascribe to these centres the parameters  $E_0^{(ax)} = 0$  and  $\Delta E^{(ax)} \simeq 0.1D$  in terms of distribution (2) but cannot estimate  $D_0^{(ax)}$  immediately from experimental data. So at  $g' = 6-8$  we observe spectra of axial  $Fe^{3+}$  centres with rhombic fluctuations.

### 3.3. Cubic $Fe^{3+}$ centres

A wide line at  $g' = 2$  was observed at 475 K. Applying the known mathematical background (Kliava 1988), we performed a computer simulation of powder-type EPR spectra for  $Fe^{3+}$  centres with  $D$  and  $E$  varying from 0 to  $0.1 \text{ cm}^{-1}$ . We found that the experimental spectrum involves responses from a set of centres with parameters  $D_0^{(cub)} = E_0^{(cub)} = 0$ ,  $\Delta D = 0.1 \text{ cm}^{-1}$  and  $\Delta E = 0.03 \text{ cm}^{-1}$  in terms of (2). The specific form of low-field tail with very weak singularity at  $g' = 3.2$  (figure 2) is characteristic of this model. So the symmetry of these centres is cubic with low-symmetry fluctuations. At 100 K the wide line at  $g' = 2$  is smeared.

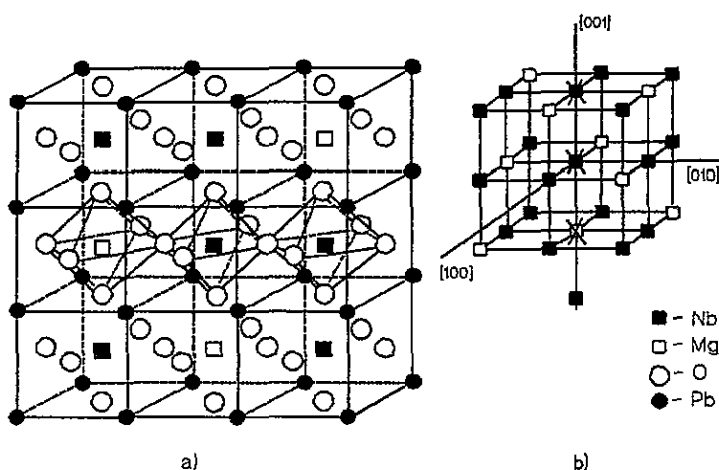


Figure 1. Ideal (stoichiometric) PMN structure (a) common view; (b) sublattice of B ions (X, X'), examples of  $Fe^{3+}$  possible positions, which may be suitable).

A narrow line with a complex structure appears (see figure 3) at 100 K. It might be attributed to a centre with  $S = \frac{1}{2}$  and an anisotropic  $g$ -tensor, e.g. an F centre. The specimen was annealed in an oxygen atmosphere at  $800^\circ\text{C}$  for 1 h to check whether the spectra are sensitive to the oxygen vacancy concentration $\dagger$ . Since the spectra of annealed specimens remained of the same intensity, the F-centre hypothesis can be rejected.

$\dagger$  The effectivity of this annealing treatment for changing the oxygen content in materials with a perovskite structure was proved earlier (Laguta *et al* (1985) and references therein).

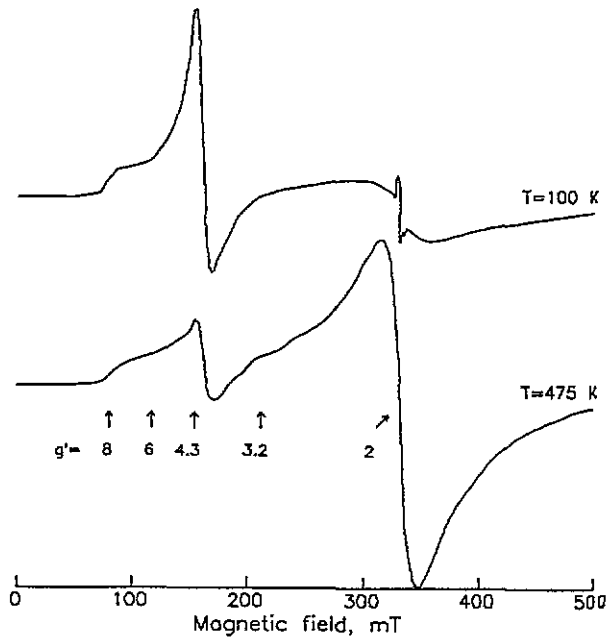


Figure 2. X-band EPR spectra of PMN ceramics doped with  $\text{Fe}^{3+}$  at 100 and 475 K. The arrows indicate effective  $g$ -values of characteristic pairs of spectra.

Another possibility for interpreting the narrow  $g' = 2$  line is to ascribe it to the isotropic  $-\frac{1}{2} \leftrightarrow +\frac{1}{2}$  transition of  $\text{Fe}^{3+}$  in a crystal field of cubic symmetry. We assume the line structure to be due to superhyperfine splitting at eight  $^{207}\text{Pb}$  nuclei (nuclear spin  $I = \frac{1}{2}$ ; isotope relative amount, 20%) place at the apices of a cube with an  $\text{Fe}^{3+}$  ion at its centre. Computer simulation of the isotropic line with a superhyperfine structure with a constant of 4 mT and a linewidth of 2 mT closely describes the experimental data (see figure 3).

#### 4. Models of $\text{Fe}^{3+}$ centres in PMN

It is known (Bonneau *et al* 1991) that in PMN the macroscopic spontaneous polarization  $P = 0$  and the average symmetry is cubic, but two mechanisms may lower the local symmetry. One of them is a chaotic distribution of  $\text{Mg}^{2+}$  and  $\text{Nb}^{5+}$  ions in B sites, contrary to the ideal 1:2 structure depicted in figure 1, i.e. structural disorder of local fields and non-compensated charges. Another mechanism is the temperature-dependent displacement of lattice ions in polar regions. As in many other perovskites, the impurity ion  $\text{Fe}^{3+}$  is expected to occupy the B site, substituting for  $\text{Mg}^{2+}$  or  $\text{Nb}^{5+}$ . As stated above, the spectra of annealed specimens remained the same; so we may not assume that the observed centres form a complex with oxygen vacancies, namely  $\text{Fe}^{3+}-\text{V}_\text{O}$ .

$\text{Fe}^{3+}$  is an S-state ion, and the mechanisms by which its spin levels split as a result of crystal fields are rather complicated. They may be found only in higher orders of the perturbation theory. Nevertheless, it was shown by Altshuler and Kozyrev (1972) that the constants  $D$  and  $E$  are proportional to matrix elements containing spherical harmonics  $Y_2^0$

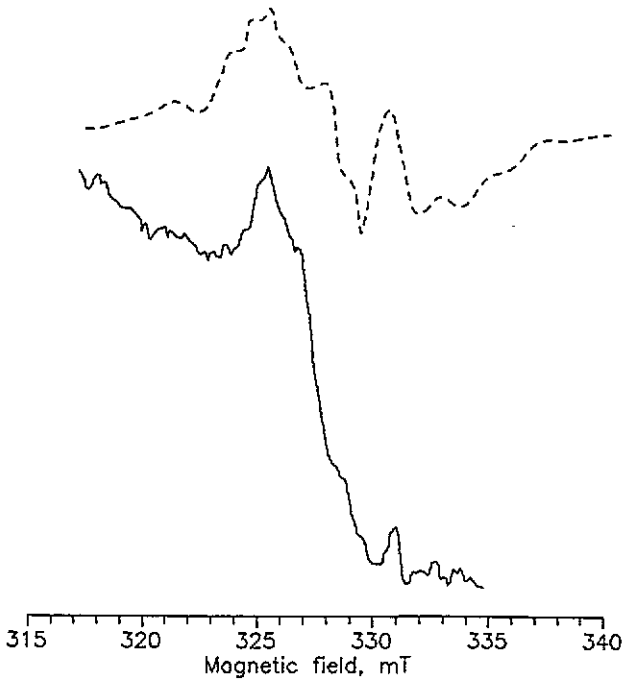


**Figure 3.** Details of the narrow  $g' = 2$  line at 100 K interpreted as the superhyperfine interaction with neighbouring  $^{207}Pb$  nuclei: —, experimental data; ---, calculated data.

and  $Y_2^2$  correspondingly and may be estimated from the equations

$$D = AZe \sum_{i=1}^n \frac{q_i}{R_i^3} (3 \cos^2 \theta_i - 1) \quad (3)$$

$$E = AZe \sum_{i=1}^n \frac{q_i}{R_i^3} [\sin^2 \theta_i \cos(2\phi_i)]$$

where  $A$  is a constant depending on the matrix elements of electron coordinate and the distance between electron terms,  $Ze$  is the paramagnetic ion charge,  $q_i$  and  $R_i$  are the charge and radius of an ion in site  $i$ ,  $\theta_i$  and  $\phi_i$  are the spherical angles of the axis connecting a paramagnetic ion with site  $i$  and  $n$  is the number of surrounding ions.

#### 4.1. B-site disorder contribution

Let us consider the contribution of the six nearest surrounding B-site cations at the apices of a right octahedron. Then, in (3),  $R_i = a$  (cubic lattice constant),  $q_i = +2$  for Mg or  $+5$  for Nb, and  $i$  varies from 1 to 6. It is convenient to calculate the dimensionless values  $D_1$  and  $E_1$ :

$$D = \gamma D_1 \quad E = \gamma E_1 \quad (4)$$

where  $\gamma = AZe/a^3$ .  $D_1$  and  $E_1$  are relative values and may be used to compare different centres. The results of calculations by (3) and (4) for all possible configurations (distribution

of Mg and Nb ions in the six B sites nearest to that occupied by Fe<sup>3+</sup>) are shown in table 1. Note that the data in the second column can be obtained by the respective redistribution of six Mg and Nb ions as nearest neighbours of the site occupied by Fe<sup>3+</sup> in figure 1(a). The relative concentrations of configurations with  $k$  nearest surrounding Mg ions ( $6 - k$  Nb ions) were calculated by the binomial law

$$P_n^k = \frac{n!}{k!(n-k)!} p^k (1-p)^{n-k} \quad (5)$$

where  $n = 6$  and  $p$  is the Mg concentration. PMN stoichiometry has  $p = \frac{1}{3}$  (see figure 1); however, since de Mathan *et al* (1991) reported regions with  $p = \frac{1}{2}$ , this case was also considered.

Table 1. Fe<sup>3+</sup> paramagnetic centres and configurations of surrounding Mg (Nb) ions. In the configuration description  $k$  is the parameter of (5), and the term 'axis' means the [100]-type cubic crystallography axis. The constants  $D_1$  and  $E_1$  are dimensionless. The last two columns show the relative concentrations of the configurations.

Centre symmetry	Configuration description	$D_1$	$E_1$	PbMg <sub>1/3</sub> Nb <sub>2/3</sub> O <sub>3</sub> concentration	PbMg <sub>1/2</sub> Nb <sub>1/2</sub> O <sub>3</sub> concentration
Cubic	(1) $k = 0$ or $k = 6$ (2) $k = 3$ (couples Mg-Nb on each axis)	0	0	0.177	0.156
Axial	(1) $k = 1$ or $k = 5$ (2) $k = 4$ or $k = 2$ (two Mg (or Nb) ions not on the same axis)	6	0	0.609	0.563
Axial	$k = 2$ or $k = 4$ (two Mg (or Nb) on the same axis)	12	0	0.082	0.94
Rhombic	$k = 3$ (two Mg (or Nb) on the same axis)	9	3	0.132	0.187

#### 4.2. Contribution of ion displacement in polar regions

Polar regions in PMN occur because of ion displacement (Bonneau *et al* 1991). As follows from the data of Colla *et al* (1992), at 100 K the correlation length is four times that at 475 K. Thus, at 100 K, the volume of the polar region is 64 times that at 475 K, and their contribution should be taken into account at low temperatures. Estimating the contributions of all shifted ions is quite complicated. However, since  $D$  and  $E$  are proportional to  $1/r^3$ , the contribution from oxygen ions strongly prevails in the first approach and may be estimated from the equation

$$D^{(pr)} = \gamma \frac{96\Delta r}{a}. \quad (6)$$

Equation (6) is a consequence of (3) and (4), where  $\Delta r$  is the oxygen shift in the [001] direction. Note that this approach is rather rough because the shifts in farthest ions are neglected, and also the real oxygen shift is more complicated than we assume in the model.

## 5. Discussion

Four types of  $Fe^{3+}$  paramagnetic centre were observed in PMN. Three of these may be described on the assumption of the  $D$  and  $E$  distribution given in (2).  $D_0$  and  $E_0$  for this distribution satisfy the conditions of cubic symmetry ( $D_0 = E_0 = 0$ ) for one type of centre, axial symmetry ( $E_0 = 0$ ) for the second type of centre, and complete rhombic symmetry ( $E_0 = \frac{1}{3}D_0$ ) for the third type. From experimental data we found the parameters of (2) for rhombic and cubic centres and calculated dimensionless constants  $D_1$  and  $E_1$  for all three types. Now that we know  $D_0^{(rh)}$  and  $D_1^{(rh)}$ , we can find  $\gamma$  from equations (3) and (4), table 1 and experimental data:  $\gamma = D_0^{(rh)}/D_1^{(rh)} = 0.0667 \text{ cm}^{-1}$ . So, at 475 K,  $D_0^{(ax)} = \gamma D_1^{(ax)} = 0.4 \text{ cm}^{-1}$  and  $\Delta E^{(ax)} = 0.1 D_0^{(ax)} = 0.4 \text{ cm}^{-1}$ . It is remarkable that for all three types of centre the values of  $\Delta E$  are very close. So we can expect the mechanism of the  $D$  and  $E$  distribution to be the same for all three centres. These fluctuations in the constants may be caused by local crystal fields as a result of the chaotic distribution of Mg and Nb ions in B sites in the farthest coordination spheres.

The response of cubic centres (wide line;  $g' = 2$ ) disappears at 100 K, which is accompanied by an increasing intensity in the  $g' = 4.3$  line of rhombic centres.  $D_0$  for the latter is  $0.4 \text{ cm}^{-1}$  while at 475 K it is  $0.6 \text{ cm}^{-1}$ ; so additional rhombic centres are assumed to occur at low temperatures. They are caused by the contribution of ion displacements in polar regions, which is essential at low temperatures. This means that those centres which are cubic at 475 K mainly become rhombic at 100 K owing to a decrease in symmetry due to ion displacements. Substituting  $D^{(or)} = 0.4 \text{ cm}^{-1}$ ,  $\gamma = 0.667 \text{ cm}^{-1}$  and  $a = 4 \text{ \AA}$  into (6), we can find the oxygen shift  $\Delta r \approx 0.25 \text{ \AA}$ . This value is in rough agreement with the data from neutron diffraction analysis (Bonneau *et al* (1991) reported a value of  $0.181 \text{ \AA}$  at 120 K), taking into account the temperature dependence of  $\gamma$ . So our simple model considering only oxygen octahedra displacement along the [001] axis may be suitable for analysis of the PMN polar behaviour by EPR.

There may seem to be disagreement between intensities of responses from observed centres and their calculated concentrations (table 1). For instance, the axial line amplitude was much less than those of rhombic and cubic lines (see figure 2). In single crystals we would observe individual orientationally dependent lines whose peak-to-peak intensity is proportional to the integral intensity (i.e. centre concentration). Meanwhile, in polycrystalline solids the spectrum is a sum of individual lines integrated over a sphere and does not have the classic Gauss or Lorentz form. The observed first derivation of absorption depends not only on the paramagnetic centre concentration but also on the linewidth and other characteristic parameters. So we may compare amplitudes of responses from centres with a similar character of response in the meaning of centre concentrations. It is seen from figure 2 that the  $g' = 4.3$  rhombic line amplitude at 100 K is approximately twice that at 475 K. At 100 K this line is the sum of responses from initially rhombic centres and centres which were cubic at 475 K, but their symmetry was reduced under polar regions. The concentrations of former and latter are fairly close (table 1). It should be noted that the calculated values of the configuration concentrations for  $p = \frac{1}{3}$  and  $p = \frac{1}{2}$  are close; so the  $p$ -value can hardly be found from EPR data.

We have shown above that the narrow line  $g' = 2$  at 100 K is a response from the  $Fe^{3+}$  cubic centre with a superhyperfine interaction on the surrounding  $^{207}\text{Pb}$  nuclei. It is essential that no spin-Hamiltonian constant distribution be characteristic for this centre; so its local symmetry is ideal cubic without any fluctuations. Ideal or homogeneous regions of PMN (see figure 1) as well as  $\text{PbMg}_{1/2}\text{Nb}_{1/2}\text{O}_3$  compositions where Mg and Nb occupy successive B sites in strict accordance with stoichiometry retain cubic local symmetry. A

weak line intensity indicates a small concentration of this centre because of the small volume of the ideal regions. This line was not observed at 475 K since it was involved in the wide cubic line. Experimental evidence showing about 10% of these ideal regions in PMN at  $T > 400$  K was obtained from NMR data by Glinchuk *et al* (1991). The present EPR data make us believe that the small volume of ideal regions is conserved down to 100 K.

## 6. Conclusions

Three types of  $\text{Fe}^{3+}$  paramagnetic centre with distributed spin-Hamiltonian constants and one type with pure cubic symmetry were observed in PMN. The disorder of cations in B sites complicated at low temperatures by ion displacement is the main origin of the symmetry decrease. The oxygen ion shift is found to be 0.25 Å, which is in agreement with previous x-ray and neutron diffraction data. Homogeneous regions with local cubic symmetry are found at 100 K.

## Acknowledgments

The authors thank V G Grachov and Y V Martynov for the software on EPR spectra simulation in polycrystalline solids.

## References

- Altshuller S A and Kozyrev B M 1972 *Elektronniy Paramagnitniy Rezonans Soedineniy Elementov Promezhutochnykh Grup* (Moscow: Nauka) p 87
- Bonneau P, Garnier P, Calvarin G, Husson E, Gavatti J R, Hewat A W and Morell A 1991 *J. Solid State Chem.* **91** 350–61
- Colla E V, Koroleva E Yu, Okuneva N M and Vakhrushev S B 1992 *J. Phys.: Condens. Matter* **4** 3671–7
- de Mathan N, Husson E, Galvarin G, Gavatti J, Hewat A and Morell A 1991 *J. Solid State Chem.* **91** 350
- Dimza V J, Sprogis A A, Kapenieks A E, Shebanov L A, Plaude A V, Stumpe R and Books M 1989 *Ferroelectrics* **90** 45
- Glinchuk M D, Laguta V V and Bykov I P 1991 *Ferroelectrics* **124** 255–60
- Kliava J 1986 *Phys. Status Solidi b* **134** 411–55
- 1988 *EPR-spektroskopiya Neuporyadochennykh Tverdyh Tel* (Riga: Zinatne) p 58
- Laguta V V, Glinchuk M D, Bykov I P, Karmazin A A and Syrnikov P P 1985 *Fiz. Tverd. Tela* **27** 2211–5
- Laguta V V, Bykov I P, Glinchuk M D, Titov A N and Andreyev E M 1990 *Fiz. Tverd. Tela* **32** 3132–4
- Wickman H H, Klein M P and Shirley D A 1963 *J. Chem. Phys.* **42** 2113–7